

**Searches for new neutral and charged scalars
with multiple top and bottom quarks in Run 2 pp
collisions at $\sqrt{s} = 13$ TeV with the ATLAS detector**

Customise this page according to your needs

Adrian Salvador Salas

July 8, 2022

An Awesome Publisher

Somewhere, something incredible is waiting to be known.

– Carl Sagan

Abstract

This thesis presents two searches for new scalars produced with the 139 fb^{-1} proton-proton collision data at a centre-of-mass energy of 13 TeV, collected by the ATLAS detector at the CERN Large Hadron collider during Run 2. Both searches are performed in multi-jet final states with one electron or muon and events categorised according to the multiplicity of jets and how likely these are to have originated from the hadronisation of a bottom quark. Parameterised feed-forward neural networks are used to discriminate between signal and background and included in maximum-likelihood fits to the data for the different mass hypotheses.

The first search is dedicated to charged Higgs bosons, predicted by various theories Beyond the Standard Model and motivated by the inadequacy of the Standard Model to explain some experimental phenomena. The work focuses on heavy charged Higgs bosons, heavier than the top quark, and decaying to a pair of top and bottom quarks, $H^\pm \rightarrow tb$, while the production is in association with a top and a bottom quark, $pp \rightarrow tbH^\pm$. The search is performed in the mass range between 200 and 2000 GeV. No significant excess of events above the expected Standard Model background is observed, hence upper limits are set for the cross-section of the charged Higgs boson production times the branching fraction of its decay. Results are interpreted in the context of hMSSM, various Mh125 scenarios and 2HDM+a.

The second search targets FCNC decays of top quarks into a new scalar decaying into a pair of bottom quarks, $t \rightarrow u/cX(bb)$, in $t\bar{t}$ events. This novel study probes for the scalar on a broad mass range between 20 and 160 GeV and branching ratios below 10^{-3} . In the case of the Higgs boson, branching ratios for $t \rightarrow u/cH$ are predicted within the Standard Model to be of $\mathcal{O}(10^{-17})/\mathcal{O}(10^{-15})$. Several Beyond the Standard Model theoretical models predict new particles and enhanced branching ratios. In particular, simple extensions involve the Froggatt-Nielsen mechanism, which introduces a scalar field with flavour charge, the so-called flavon, featuring flavour violating interactions. As no significant excess is observed, upper limits for both FCNC decays $t \rightarrow uX$ and $t \rightarrow cX$ are computed. In addition, limits are set for the process involving the Standard Model Higgs.

Contents

Abstract	v
Contents	vii
Introduction	1
THEORETICAL AND EXPERIMENTAL SETUP	3
1 The Standard Model of Particle Physics and beyond	5
1.1 The Standard Model of Particle Physics	5
1.1.1 Particle content of the Standard Model	5
1.1.2 Interactions of the Standard Model	8
1.1.3 Quantum Chromodynamics	10
1.1.4 Electroweak theory	14
1.1.5 Spontaneous symmetry breaking and the Higgs mechanism	16
1.1.6 Flavour Changing Neutral Currents interactions	24
1.2 Standard Model measurements and top physics	25
1.2.1 Experimental measurements	25
1.2.2 Top quark physics	28
1.2.3 FCNC measurements	30
1.2.4 Open questions	30
2 The ATLAS experiment at the LHC	33
3 Physics simulation of proton collisions	35
4 Object reconstruction	37
5 Machine learning	39
CHARGED HIGGS BOSON WITH $H^\pm \rightarrow tb$ SEARCH	41
NEUTRAL SCALAR PRODUCED IN $t \rightarrow qX$ WITH $X \rightarrow b\bar{b}$ SEARCH	43
APPENDIX	45
Bibliography	47

Introduction

The discovery of the Higgs boson in 2012 by ATLAS and CMS [1, 2] is one of the most recent historic milestones in the field of particle physics. CERN hosts the LHC, which physics' program included the hunt of the Higgs boson. After this achievement, all particles predicted by the Standard Model are discovered, the theory which describes the fundamental particles and their interactions. Nevertheless, the ATLAS experiment continues to scrutinise the Standard Model of particle physics by analysing the ever-increasing amount of particle collisions delivered by the LHC. There are many phenomena not covered by the current theory and any measurement that deviates from the predictions or any hint of a new particle will lay the foundation for a new path in particle physics.

The theory of the Standard Model has successfully guided the experiments with the prediction of particles and precise values of their interactions. However, no other theory has been able to explain the tiny deviations with respect to the theory or filled the gaps that the Standard Model does not even contemplate. Known tensions with respect to the theory predictions are regarding the lepton universality [3] or the measurement of the anomalous magnetic dipole momentum of the muon ($g-2$) [4]. On the other hand, the theory fails to cover gravity, the neutrino masses, dark matter... although one of the most compelling concerns regarding the Standard Model is known as the hierarchy problem, the seemingly unnatural fact that the Higgs mass, yet not having any constrain in the theory, appears to be at the electroweak scale. One of the possible theoretical solutions consists in an expansion of the Standard Model which spawns additional scalar particles. If the Higgs sector is built with one extra doublet (Two Higgs Doublet Models), a total of five scalars are predicted instead, including Higgs bosons with electrical charge. Another similar feature of the Standard Model is known as the flavour problem, as fermions can be grouped in three families with different mixing patterns, which is also seen as arbitrary choice. This feature can be explained by introducing a broken flavour symmetry spawning a new particle, the flavon, which introduced flavour violating interactions. The presence of flavour-changing neutral current (FCNC) interactions is heavily suppressed in the Standard Model, way below the available sensitivity. These interactions are hence very sensitive to new physics as any observed interaction cannot be explained by the Standard Model.

In this thesis, a direct search for charged Higgs bosons heavier than the top quark and a direct search for neutral scalars lighter than the top quark are presented. The charged Higgs process is searched in the 200 – 2000 GeV mass range produced in association with top and bottom quarks and decaying into a top-bottom, while the neutral scalar is searched in the 20 – 160 GeV mass range produced in the FCNC decay of a top quark involving a c - or a u -quark, and finally decaying to a pair of b -quarks. Limits on the production of charged Higgs bosons in the same channel have been previously obtained by ATLAS with only the data from 2015 and 2016 for $H^\pm \rightarrow tb$ in the 200 – 2000 GeV mass range [5], and more recently by CMS in the

200 – 3000 TeV GeV mass range using the full Run-2, setting upper limits at 95% confidence level on the production cross section of $2.9 - 0.070$ pb and $9.6 - 0.01$ pb respectively. On the other hand, both ATLAS and CMS have searched for the top FCNC decay into the SM Higgs, $t \rightarrow qH$ with q being either a c - or u -quark. Both ATLAS and CMS have performed multiple measurements on this process, the most recent from ATLAS being in the $H \rightarrow \tau\tau$ channel [6] while the CMS results with 137 fb^{-1} data combines several channels and sets the limits to $t \rightarrow uH < 0.079$ and $t \rightarrow cH < 0.094$ [7]. However, these results are for the SM Higgs and the generic signature of a scalar lighter than the top quark presented in this work is uncovered in literature.

Both searches performed in this thesis are performed using the full Run-2 proton-proton collisions collected by the ATLAS experiment from 2015 to 2018 at a center-of-mass energy of 13 TeV. Events are selected to have either one electron or muon and multiple jets, including those originated from the hadronisation of a bottom quark. Results are extracted by means of binned maximum-likelihood fits of the different simulated signal and SM backgrounds to the recorded data. The fit is performed on a discriminant obtained by combining several kinematic variables through the training of parameterised feed-forward neural networks, developed to optimise the sensitivity by separating signal and background events.

The document is structured into three main parts: The first part describes the theoretical and experimental setup, while the second part includes the $H^\pm \rightarrow tb$ analysis while the third part includes the $t \rightarrow qX$ analysis, both with a detailed description of the strategy and their results. Chapter 1 focuses on the Standard Model and the models that motivate the searches. Chapter 2 provides an overview of the LHC and the ATLAS experiment. Chapters 3 and 4 present the essential aspects of the simulation and reconstruction of simulated proton-proton collisions, while Chapter 5 presents the machine learning techniques and statistical tools used in the different analyses.

THEORETICAL AND EXPERIMENTAL SETUP

The Standard Model of Particle Physics and beyond

1

The Standard Model (SM) of particle physics [8–10] is the theoretical framework that so far better describes subatomic particles and their interactions. It is a Quantum Field Theory (QFT) and since its initial development in the 1960's, the model has been overwhelmingly successful and guided many experimental achievements including the discovery of the top quark [11, 12] in 1995 and the Higgs boson at the LHC in 2012 [1, 2]. Regardless of its success, there are known phenomena not covered in the model and other questions which clearly point to the need of a new theories.

This chapter starts with an overview of the SM, building it with its mathematical formalism, and presenting a summary of the particle content and their interactions as of yet. Then, it continues with a summary of the current success of the theory, but also shortcomings and alternative models that could serve as solutions. The focus is given to models that include charged Higgs bosons or top FCNC interactions involving a scalar.

Throughout this dissertation, natural units are used: the speed of light and the reduced Plank constant are set to unity ($c = \hbar = 1$), electric charges are expressed in units of the electron electric charge ($-e$) and masses are expressed in terms of energy (eV). Within the theoretical developments in this chapter, the Einstein's summation convention is used by default.

1.1 The Standard Model of Particle Physics

From the mathematical point of view, the SM is a renormalisable non-abelian gauge QFT based on the symmetry group,

$$SU(3)_C \otimes SU(2)_L \otimes U(1)_Y \quad (1.1)$$

where $SU(3)_C$ is the group described by Quantum Chromodynamics (QCD) [13] that represents the strong interactions of colored quarks and gluons (strong force), while $SU(2)_L \times U(1)_Y$ is the inclusive representation of both electromagnetic (EM) and weak interactions described by the ElectroWeak (EW) theory [8, 9, 14]. The SM describes all the interactions between elementary particles except gravity, for which no renormalisable QFT has been formulated so far. The following sections, introduce the particles of the SM and the theories that describe their interactions.

1.1.1 Particle content of the Standard Model

In the SM, elementary particles are described as excitations of quantum fields. There are two main classes of particles within the theory: *fermions* and *bosons*. The main

difference between the two is the spin: fermions have half-integer spin and therefore obey the Pauli exclusion principle [15], while bosons have integer spin.

Fermions

Fermions can be divided further into two categories: quarks and leptons, based on their interactions, or their charges. Both types manifest in EW interactions, having a weak isospin $T_3 = \pm 1/2$ while only the quarks experience the strong interaction. Quarks have a fractional electric charge $|Q| = 2/3$ or $1/3$, and the *colour*. The last one is the charge associated to the strong interaction and its values are denoted as *red*, *green* and *blue*. Table 1.1 presents a summary of the fundamental fermions and their characteristics.

Table 1.1: Table of the different quarks and leptons of the SM grouped in families with their mass and electric charge according to the Particle Data Group [16]. The uncertainties on the electron and the muon masses are below 10^{-10} and 10^{-6} MeV, respectively. The anti-matter states are not shown.

Generation	Name	Symbol	Mass	Charge
Quarks				
1 st	Up	u	$2.15^{+0.49}_{-0.26}$ MeV	+2/3
	Down	d	$4.67^{+0.48}_{-0.17}$ MeV	-1/3
2 nd	Charm	c	1.27 ± 0.02 GeV	+2/3
	Strange	s	$93.4^{+8.6}_{-3.4}$ MeV	-1/3
3 rd	Top	t	172.69 ± 0.30 GeV	+2/3
	Bottom	b	$4.18^{+0.03}_{-0.02}$ GeV	-1/3
Leptons				
1 st	Electron	e^-	0.511 MeV	-1
	Electron neutrino	ν_e	< 1.1 eV 90% CL	0
2 nd	Muon	μ^-	0.106 GeV	-1
	Muon neutrino	ν_μ	< 0.19 MeV 90% CL	0
3 rd	Tau	τ^-	1776.86 ± 0.12 MeV	-1
	Tau neutrino	ν_τ	< 18.2 MeV 95% CL	0

There is a total of six quark types, named *flavours*, and are split into three generations. The first generation consists in the *up* and the *down* quark, the former with $Q = +2/3$ and $T_3 = +1/2$, while the latter $Q = -1/3$, $T_3 = -1/2$ and a slightly lower mass. The next two generations are copies of the first one with increasing mass, with a pair of a *up*-type quark and a *down*-type quark. The second family consists in *charm* and *strange* quarks, and the third of *top* and *bottom* quarks. In addition, all of the six quark flavours have antimatter states with the same mass, but opposite quantum numbers, as an example, an anti-*up*-type quark has $Q = -2/3$, $T_3 = -1/2$ and can carry anti-*red* colour.

Leptons are also similarly divided in six different types and in three separate generations named *electron* (e), *muon* (μ) and *tau* (τ), also with increasing mass.

Each generation contains a lepton with $Q = -1$ and $T_3 = +1/2$ named after its generation, and an associated electrically neutral lepton with $T_3 = -1/2$ named neutrino (ν). The neutrino is assumed to be massless in the formulation of the SM, however the phenomena of neutrino oscillations is experimental proof of them actually having very small, but non-zero, mass values. This apparent failure of the theory is discussed in Section 1.2.4. As before, the associated antimatter states have the same mass but opposite quantum numbers.

All the stable SM matter in the universe is constituted by the massive particles of the first generations of quarks and leptons, as the heavier versions eventually decay to lighter ones through their disclosed interactions. While it is possible to observe free leptons, quarks exist only in bound states, or hadrons, like the neutron or the proton. This is a feature of the strong interaction under the name of confinement, discussed in Section 1.1.3. Only colour-less bounded states are observable then, and can be built from three quarks with overall half-spin, named baryons, or by two quarks with integer spin, named mesons.

In the context of particle physics, the formulation of the classical Lagrangian, \mathcal{L} , is used to describe physics systems. A generic free fermion field ψ with mass m , can be described by the Dirac Lagrangian,

$$\mathcal{L} = \bar{\psi}(i\gamma^\mu\partial_\mu - m)\psi, \quad (1.2)$$

where γ^μ are Dirac matrices and ∂_μ is the four-momentum derivative.

Bosons

Particles with integer spin are referred to as bosons. The bosonic sector with spin-1 gauge fields are force carriers that naturally follow from imposing the requirement of local gauge invariance on Equation 1.2 under symmetry groups, in this case Equation 1.1. In Section 1.1.2 the nature and origin of the gauge bosons will be detailed. Table 1.2 presents a summary of the bosons of the SM.

Table 1.2: Table of the different bosons of the SM with their mass and electric charge according to the Particle Data Group [16]. The Higgs boson has spin 0 and does not mediate an interaction, while the rest have spin 1 and mediate an interaction.

Name	Mass [GeV]	Charge	Interaction
Photon (γ)	0	0	Electromagnetic
Z	91.1876 ± 0.0021 GeV	0	Weak
W^\pm	80.377 ± 0.012 GeV	± 1	
Gluon (g)	0	0	Strong
Higgs	125.25 ± 0.17 GeV	0	-

In summary, the photon (γ) is the carrier of the electromagnetic force, being a massless and electrically neutral particle. The weak force carriers are the W^+ , W^- and Z bosons, all massive with the Z boson being electrically neutral and the W^\pm

with either $Q = \pm 1$. Gluons (g) are the strong force carriers which are massless and with no electric charge. Instead, there are eight different gluons representing each possible colour exchange.

The SM also includes a neutral spin-0 particle, or *scalar*, the Higgs boson. The Higgs field is responsible for all SM particles acquiring mass through the Higgs mechanism, as described in Section 1.1.5. The kinematics of a generic scalar ϕ with mass m , is described by the Klein-Gordon Lagrangian,

$$\mathcal{L} = \frac{1}{2} \partial^\mu \phi \partial_\mu \phi - m^2 \phi^2 \quad (1.3)$$

Charged scalars can be described instead through a complex field and the expression of the Lagrangian is slightly modified,

$$\mathcal{L} = \partial^\mu \phi \partial_\mu \phi^* - m^2 \phi \phi^* \quad (1.4)$$

Vector fields A^μ , which represent spin-1 bosons, are described by the Proca Lagrangian,

$$\mathcal{L} = -\frac{1}{4} F^{\mu\nu} F_{\mu\nu} + \frac{1}{2} m^2 A^\mu A_\mu \quad (1.5)$$

with $F^{\mu\nu} = \partial^\mu A^\nu - \partial^\nu A^\mu$ the field strength tensor. In the case of massless particles, the previous expression with $m = 0$ is known as the Maxwell Lagrangian.

1.1.2 Interactions of the Standard Model

The Lagrangian of the SM is defined to be locally invariant to the Equation 1.1 symmetry group, condition that generates and defines the interactions of the corresponding particles as representations of the symmetry transformations. For a generic Lagrangian, the physical system can have symmetries, so its Lagrangian is invariant under different kind of transformations. These transformations can be time-space independent, called global transformations, or dependent, called gauge or local transformations. Any invariant transformation of a Lagrangian describes a physical system which conserves a physical quantity, as described by the Noether theorem [17]. Then, the interactions are introduced in the Lagrangian as additional terms by promoting an already existing global symmetry, ϕ , of the Lagrangian to a local gauge symmetry, $\phi(x)$. The physical motivation behind introducing gauge symmetries is to be able to describe vector bosons in QFT. The procedure expands the theory with additional fields that mediate the resulting interactions, which properties depend on the characteristics of the symmetry group.

An example of the process is shown in the following, to afterwards derive the SM interactions of the strong and electroweak sectors.

Gauging a symmetry to interaction

A general global transformation θ which acts on the field ψ is described as,

$$\psi \rightarrow e^{ig\theta^a T^a} \psi \quad (1.6)$$

with g the coupling constant and T^a the generators of the Lie group associated to the transformation (like $SU(n)$ or $U(n)$), with a ranging from 1 to $n^2 - 1$, for the corresponding number of the Lie algebra, $n > 1$. The generators can be characterised by their commutation relation,

$$[T^a, T^b] = if^{abc} T^c \quad (1.7)$$

where f^{abc} are the structure constants of the group. Following Noether's theorem, there are as many conserved quantities as generators of the Lagrangian's symmetries. As an example, it is straightforward to see that a Lagrangian like Equation 1.2 is invariant to a $U(1)$ transformation where θ is just a constant and hence, a constant phase change. One can obtain the current, j^μ , that is conserved, $\partial_\mu j^\mu = 0$,

$$j^\mu = \bar{\psi} \gamma^\mu \psi \quad (1.8)$$

and the conserved charge,

$$Q = \int d^3x j^0 = \int d^3x \psi^\dagger \psi \quad (1.9)$$

With some algebra and introducing solutions in momentum space, ψ can be interpreted as annihilating a fermion and creating an anti-fermion (ψ^\dagger the other way around) in the Fock space and then, this product becomes the difference of the number of fermion and anti-fermion leading to the conservation of the fermion number.

Promoting the global symmetry to a local symmetry is done by introducing locality in the θ transformation, $\theta \rightarrow \theta(x)$, which introduces new $\partial_\mu \theta$ terms in the Lagrangian. A way to counter the new terms and, hence, keep the Lagrangian invariant, is to introduce gauge vector fields A_μ^a , following Yang-Mills theory [18]. In the most generalised approach, there have to be as many A_μ^a as generators of the symmetry, that transform as,

$$A_\mu^a \rightarrow A_\mu^a + \partial_\mu \theta^a + gf^{abc} A_\mu^b \theta^c \quad (1.10)$$

Note that the last term proportional to the structure constant is relating the gauge field to the conserved symmetry charge. The next step is to replace the standard derivative in the Lagrangian by the covariant derivative,

$$D_\mu \equiv \partial_\mu - igT^a A_\mu^a \quad (1.11)$$

The final ingredient is to complete the Lagrangian with the kinematic Lagrangian for the massless vector fields, the Maxwell Lagrangian from Equation 1.5 with a slightly different field strength tensor,

$$F_{\mu\nu}^a = \partial_\mu A_\nu^a - \partial_\nu A_\mu^a + gf^{abc} A_\mu^b A_\nu^c \quad (1.12)$$

The last term is present only for non-abelian symmetry groups, since it is proportional to the structure constants, and has huge consequences in the resulting interactions as discussed in the next Section. Another remark is that the gauge fields have to be massless, as a mass term proportional to $A_\mu^c A^{\mu c}$ is not gauge invariant.

As an example, the promotion of the global $U(1)$ symmetry seen in Equation 1.2 results in the upgraded Lagrangian,

$$\begin{aligned} \mathcal{L} &= \bar{\psi}(i\gamma^\mu D_\mu - m)\psi - \frac{1}{4}F_{\mu\nu}F^{\mu\nu} \\ D_\mu &\equiv \partial_\mu - igA_\mu \\ F_{\mu\nu} &\equiv \partial_\mu A_\nu - \partial_\nu A_\mu \end{aligned} \quad (1.13)$$

introducing just one massless gauge field that interacts with the field ψ . The interaction term between the two fields is $g\bar{\psi}\gamma^\mu A_\mu\psi$, hidden in the covariant derivative definition and proportional to the coupling constant g .

The Lagrangian of the SM is built from imposing local invariance under $SU(3)_C$ transformations, which leads to strong interactions; and $SU(2)_L \times U(1)_Y$ transformations, which brings EW interactions,

$$\mathcal{L}_{SM} = \mathcal{L}_{QCD} + \mathcal{L}_{EW} \quad (1.14)$$

After this introduction on field theory, the theories of the two orthogonal sectors can now be described and then, the mechanism to introduce mass terms in the Lagrangian, the spontaneous symmetry breaking.

1.1.3 Quantum Chromodynamics

The quantum field theory that describes quarks, gluons and their interactions is named *quantum chromodynamics*. Each quark has an internal degree of freedom, the colour charge, and it is defined by a triplet of fields,

$$q = \begin{pmatrix} q_{\text{red}} \\ q_{\text{blue}} \\ q_{\text{green}} \end{pmatrix} \quad (1.15)$$

where each of the components is a Dirac spinor associated to the corresponding colour state (red, blue and green). In addition, there are a total of six quarks, so the fields are labelled as $q_{f\alpha}$ with f indicating the quark flavour ($f = u, d, c, s, t, b$) and α the colour. Note that there is an anti-quark of each flavour carrying an anti-colour charge.

The theory is based on the $SU(3)$ symmetry group, which algebra is characterised by the non-abelian commutation relation from Equation 1.7 with a total of eight generators, T^a . The generators can be written as $T^a = \lambda^a/2$ where λ^a denote the Gell-Mann matrices [19]. Because of the eight generators, the interaction is mediated by a total of eight gauge bosons, called gluons G_μ^a . There are different matrix representation for the colour states of the gluons, following with the Gell-Mann matrices, taking,

$$\lambda^1 = \begin{pmatrix} 0 & 1 & 0 \\ 1 & 0 & 0 \\ 0 & 0 & 0 \end{pmatrix} \quad (1.16)$$

and applying it to a general quark triplet like Equation 1.15, it can be seen that the transformation switches the red and blue charges. To do so, the gluon has to carry a colour/anti-colour pair, to be able to "remove" the red charge (r) and "add" the blue charge (b), and the other way around. There are nine possible combinations of colour/anti-colour pairs, which can be used to re-write the λ^1 transformation as,

$$\frac{r\bar{b} + b\bar{r}}{\sqrt{2}} \quad (1.17)$$

known as the first state of the gluon colour octet. The rest of the states are equivalent to the other Gell-Mann matrices and all conserve the three different colour flows.

The QCD Lagrangian can be obtained from modifying the the Dirac Lagrangian (Equation 1.2) to achieve gauge invariance under $SU(3)_C$ transformations, following the definitions from Section 1.1.2. The resulting Lagrangian is,

$$\begin{aligned} \mathcal{L}_{QCD} &= i \sum_f \bar{q}_f \gamma^\mu D_\mu q_f - \frac{1}{4} G_{\mu\nu}^a G^{a\mu\nu} \\ D_\mu &\equiv \partial_\mu - i g_s T^a G_\mu^a \\ G_{\mu\nu}^a &\equiv \partial_\mu G_\nu^a - \partial_\nu G_\mu^a + g_s f^{abc} G_\mu^b G_\nu^c \end{aligned} \quad (1.18)$$

with g_s being the strong force coupling constant and where the covariant derivative has been introduced with the G_μ^a gluons fields, together with the kinematic term for the gluons, with the gluon tensor $G_{\mu\nu}^a$. As described in Section 1.1.2, gluons are massless because the term in the Lagrangian is not gauge invariant. Notice that the masses of the quarks are also not present, not because it would break the symmetry, but for convention. The masses in the SM come from the electro-weak sector. Another remark is that the addition of a charge conjugation and parity symmetry

(CP) violating interaction term is allowed under local gauge invariance, but such an interaction has been experimentally observed to be effectively zero [20].

The possible interactions in the Lagrangian are shown in Figure 1.1, consisting of couplings between quarks and gluons¹, and three- and four-point gluon self-interactions. As foreshadowed in Section 1.1.2, for non-abelian groups the gauge bosons have the self-interacting terms in the tensor.

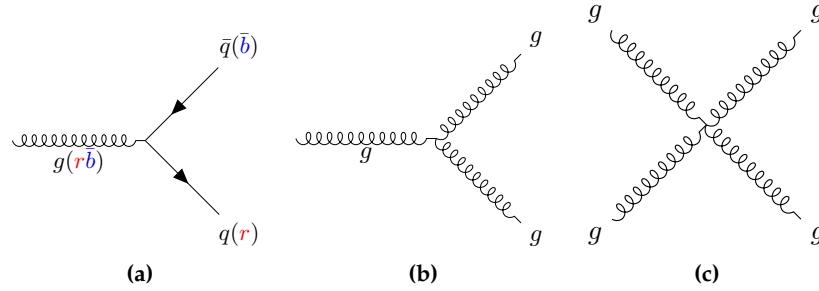


Figure 1.1: Vertices allowed in QCD: (a) quark-gluon coupling, (b) three-point gluon self-coupling, and (c) four-point gluon self-coupling. The color charge is depicted in the quark-gluon vertex to depict an example of the interaction.

There are two more important characteristics of this theory: asymptotic freedom and confinement [21, 22]. Asymptotic freedom refers to the fact that at very high energies (in momentum transfer), or short distances, quarks and gluons interact weakly with each other allowing predictions to be obtained using perturbation theory. Confinement is the name given to the impossibility of directly observing quarks, only confined in hadrons, which are colorless composite states². The idea is that for high distances, the strong coupling becomes larger, so when the distance between two quarks is increased, the energy of the gluon field is larger, up to the point to create from the vacuum a quark/anti-quark pair and thus forming a new hadron. These characteristics arise from the non-abelian nature of the symmetry, which prompt the coupling to decrease with the energy of the interaction.

Running coupling


To understand the fact that the couplings can vary with the energy, the QFT renormalisation and regularisation procedures have to be introduced. The quantity known as the matrix amplitude has to be computed for the prediction of physical quantities of a given process. Observables are actually proportional to the square sum of the amplitude of every possible Feynman diagram that yields the same initial and final particles of the process to be predicted. However, the computation in diagrams with loops spawns the integration for all possible four-momentum of the virtual particles involved, which are divergent. Nevertheless, these divergencies can be isolated with regularisation techniques, which renders them finite by introducing

¹ Equivalent to the interaction obtained from the gauge $U(1)$ symmetry.

² Color singlets are quantum states that are invariant under all eight generators of $SU(3)$, and therefore carry vanishing values of all colour conserved charges.

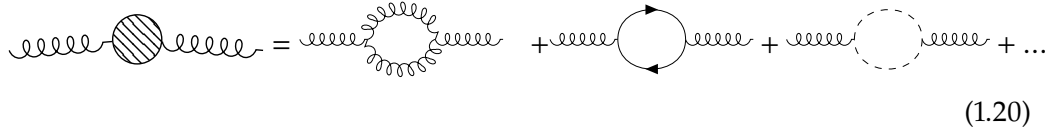
a parameter Λ such that only for a given value of the parameter the divergence is recovered. This allows the computation of any quantity in terms of the *bare* quantities appearing in the Lagrangian, such as masses and couplings, along the regularisation parameter. The other key point is renormalisation, from the idea that the physical quantities measured in experiments (masses and couplings), are different from the bare quantities (masses and couplings that appear in the lagrangian). Therefore, one has the freedom to apply renormalisation conditions which cause the expressions to depend only on the physical quantities if the theory is renormalisable, removing the divergent sources.

As an example, to compute the gluon two-point function, an infinite sum of loop contributions is needed,



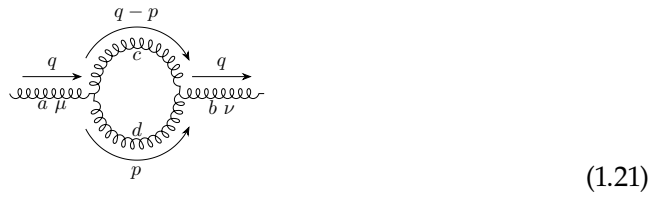
$$\text{wavy line} \circ \text{wavy line} = \text{chain of wavy lines} + \text{wavy line} \circ \text{shaded circle} + \text{wavy line} \bullet \text{shaded circle} + \dots \quad (1.19)$$

Focusing on the one loop contribution, the result is obtained at first order from three different diagrams,



$$\text{wavy line} \circ \text{shaded circle} = \text{gluon loop} + \text{quark loop} + \text{ghost loop} + \dots \quad (1.20)$$

which includes the loop involving gluons, quarks and a third one with a new propagator, the ghost. This propagator is a regularisation artifact to compensate unphysical degrees of freedom³. Focusing on the gluon loop contribution,



$$\text{Diagram (1.21)} \quad (1.21)$$

prompts in its computation with Feynman rules a badly divergent integral,

$$\frac{1}{2} g_s^2 f^{acd} f^{bcd} \int \frac{d^4 p}{(2\pi)^4} \frac{1}{(q-p)^2 + i\epsilon} \frac{1}{p^2 + i\epsilon} \left[g^{\mu\alpha} (p-2q)^\beta + g^{\alpha\beta} (q-2p)^\mu + g^{\beta\mu} (p+q)^\alpha \right] \left[\delta_\alpha^\nu (p-2q)_\beta + g_{\alpha\beta} (q-2p)^\nu + \delta_\beta^\nu (p+q)_\alpha \right] \quad (1.22)$$

which can be worked around with a regularisation constant μ ,

³ There are other methods to avoid the unphysical degrees of freedom, as choosing a physical gauge in the axial direction.

$$\int \frac{d^4 p}{(2\pi)^4} \rightarrow \int \frac{d^D p}{(2\pi)^D} \mu^{2\varepsilon}.$$

and $D = 4 - 2\varepsilon$ with later $\varepsilon \rightarrow 0$. After the computation of all main contributions, the divergent term can be summarised as,

$$\frac{g_s^2}{24\pi} [11n_c - 2n_f] \frac{1}{\varepsilon} + \mathcal{O}(g_s^4) \quad (1.23)$$

with n_c the number of colours, n_f the number of quark flavours and $\varepsilon \rightarrow 0$ the condition to recover the original divergence. Hence the bare coupling constant can be rewritten to account for this divergence, completing the regularisation process for the gluon self-energy.

The final strong coupling constant is commonly given by,

$$\alpha_s(Q^2) = \frac{12\pi}{(11n_c - 2n_f) \log \frac{Q^2}{\Lambda_{\text{QCD}}^2}} \quad (1.24)$$

which depends on the energy scale Q at which is evaluated and Λ_{QCD} the infrared cutoff scale which sets the validity of the perturbative regime of QCD. As $n_c = 3$, for $n_f < 16$ the coupling constant decreases with the energy scale, the very feature of QCD that causes asymptotic freedom and confinement.

1.1.4 Electroweak theory

The quantum field theory that describes both the electromagnetic and weak interactions is named *electroweak* theory. The theory is based on the $SU(2)_L \otimes U(1)_Y$ symmetry group⁴, which is a product that yields a non-abelian group, like $SU(3)_C$, and chiral. It will spawn four mediators, as the number of generators. The symmetry spontaneously breaks down through *symmetry breaking*, giving rise to the electromagnetic interaction, mediated by the photon, and to the weak interaction, mediated by the Z and W^\pm bosons. This process is described by the *EW symmetry breaking* (EWSB), which occurs at ~ 100 GeV, defined as the EW scale, and after which only the $U(1)_Q$ symmetry is unbroken, . The process of the EWSB, and the resulting effects are described in more detail in Section 1.1.5.

The interactions for the EW sector can be obtained following the procedure described in general in Section 1.1.2, already used in Section 1.1.3 for QCD. First, only left-handed fermion fields interact via the weak interaction⁵, transforming as doublets under $SU(2)_L$, whereas right-handed fermion fields do not interact weakly and thus transform as singlets,

⁴ L refers to the left-handed chirality and Y to the weak hypercharge

⁵ As a consequence, parity can be violated in weak interactions [23, 24].

$$\begin{aligned}\psi_L^i &= \begin{pmatrix} \ell_L^i \\ \nu_L^i \end{pmatrix}, \begin{pmatrix} u_L^i \\ d_L^i \end{pmatrix} \\ \psi_R^i &= \ell_R^i, u_R^i, d_R^i\end{aligned}\quad (1.25)$$

with i corresponding to the number of the generation. Fields with subscripts L/R are left- and right-handed fields that can be defined through the chirality operators P_L and P_R , projecting a generic field into only its left- and right-handed components, respectively,

$$\begin{aligned}\psi_L &= P_L \psi = \frac{1}{2}(1 - \gamma_5)\psi \\ \psi_R &= P_R \psi = \frac{1}{2}(1 + \gamma_5)\psi\end{aligned}\quad (1.26)$$

with γ_5 defined from the Dirac matrices $\gamma_5 \equiv i\gamma^0\gamma^1\gamma^2\gamma^3$. Notice that there are no right-handed fields associated to the neutrinos. This convention exists to avoid the prediction of right-handed neutrinos, which would not interact with any of the forces described in the SM.

The $SU(2)_L$ group consists of three generators \hat{T}_i , which can be written as $\hat{T}_i = \sigma_i/2$ where σ_i denotes the Pauli matrices. Also, the quantum number associated is the weak isospin, T . On the other side, the $U(1)_Y$ group introduces the weak hypercharge quantum number, Y . After EWSB, the Gell-Mann-Nishijima equation relates Y to the third component of the weak isospin operator, T_3 and the electric charge Q ,

$$Q = Y + T_3 \quad (1.27)$$

Regarding the EW Lagrangian, four gauge fields need to be introduced to achieve invariance under the $SU(2)_L \otimes U(1)_Y$: $W_{\mu\nu}^i$ ($i=1,2,3$) from $SU(2)_L$, and B_μ from $U(1)_Y$. The resulting Lagrangian is,

$$\begin{aligned}\mathcal{L}_{EW} &= i \sum_{f=l,q} \bar{f}(\gamma^\mu D_\mu)f - \frac{1}{4}W_{\mu\nu}^i W^{i\mu\nu} - \frac{1}{4}B_{\mu\nu}B^{\mu\nu} \\ D_\mu &\equiv \partial_\mu - ig\frac{\sigma}{2}W_\mu^i - ig'\gamma B_\mu \\ W_{\mu\nu}^i &\equiv \partial_\mu W_\nu^i - \partial_\nu W_\mu^i + g\epsilon^{ijk}W_\mu^j W_\nu^k \\ B_{\mu\nu} &\equiv \partial_\mu B_\nu - \partial_\nu B_\mu\end{aligned}\quad (1.28)$$

with ϵ^{ijk} the Levi-Civita symbol, an antisymmetric tensor defined as $\epsilon^{ijk}\epsilon_{imn} = \delta_m^j\delta_n^k - \delta_n^j\delta_m^k$ with $i, j, k, l, m, n \in [1, 2, 3]$. Also, the $W_{\mu\nu}^i$ and $B_{\mu\nu}$ field tensors are defined to introduce the additional kinetic terms to the Lagrangian. The former contains a quadratic piece, due to the non-abelian nature of $SU(2)_L$, hence the full

Lagrangian contains cubic and quartic self-interactions, as seen for the gluons in QCD. In contrast, the coupling constant g increases rapidly with the energy scale. As encountered before, mass terms for the gauge boson would break the gauge invariance. In this case, terms for the fermion masses would also break the symmetry as they would mix left- and right-handed fields, which transforms distinctively under $SU(2)_L$.

Summing all the interactions described, the SM Lagrangian for all the fermions before EWSB becomes,

$$\begin{aligned}\mathcal{L}_{SM} = & \sum_f \sum_{\psi=L, e_R, Q_L, u_R, d_R} i\bar{\psi}^f \gamma^\mu D_\mu \psi^f \\ & - \frac{1}{4} G_{\mu\nu}^a G^{a\mu\nu} - \frac{1}{4} W_{\mu\nu}^i W^{i\mu\nu} - \frac{1}{4} B_{\mu\nu} B^{\mu\nu} \\ D_\mu = & \partial_\mu - ig_s T^a G_\mu^a - ig \frac{\sigma^i}{2} W_\mu^i - ig' Y B_\mu\end{aligned}\quad (1.29)$$

1.1.5 Spontaneous symmetry breaking and the Higgs mechanism

The model described so far cannot reproduce measured results, first of all the different fermions and the weak force mediators have mass and second, the $SU(2)_L \times U(1)_Y$ symmetry is not preserved in nature. Even if somehow the EW gauge bosons are allowed to have mass, it leads to the lack of renormalisability and the violation of unitarity. Renormalisation is a collection of techniques that allows the computation of measurable observables in QFT, managing the different sources of infinities within the theory like those from self-interactions. Unitarity is needed more in general in quantum mechanics, to ensure proper time-evolution predictions of a quantum state. The longitudinal component of the massive boson is the cause of the problem, as in a boosted frame in which $p^\mu = (p^0, 0, 0, |\mathbf{p}|)$, the parallel polarisation component of a massive boson is $\epsilon_\mu = (|\mathbf{p}|/m, 0, 0, p^0)$, growing indefinitely with the energy of the system. When computing the cross-section of the corresponding boson scattering, the value will indefinitely grow breaking the mentioned unitarity. If computed explicitly for the W^\pm bosons, the energy scale where this happens is around the TeV scale, pointing to a fundamental problem in the theory to describe that scale.

The solution is provided by the EWSB and the Higgs-Englert-Brout mechanism, discussed next, after showing the spontaneous symmetry breaking process for a simple gauge theory.

How to break a symmetry

Spontaneous symmetry breaking is a phenomenon where a symmetry of the theory is unstable and the vacuum, or fundamental state, is degenerate. In the process, new interactions appear and a field obtains a non-zero vacuum expectation value.

The topic is broad as there are many symmetries and representations to potentially break, to illustrate the mechanism for the SM, let's consider a system with a scalar field ϕ , a gauge field A_μ , and the following Lagrangian with a gauge symmetry,

$$\begin{aligned}\mathcal{L} &= (D^\mu \phi)^\dagger D_\mu \phi - V(\phi) - \frac{1}{4} F_{\mu\nu} F^{\mu\nu} \\ D_\mu &\equiv \partial_\mu - ig A_\mu \\ F_{\mu\nu} &\equiv \partial_\mu A_\nu - \partial_\nu A_\mu\end{aligned}\tag{1.30}$$

with a general potential $V(\phi)$ given by,

$$V(\phi) = \frac{1}{2} \mu^2 \phi^\dagger \phi + \frac{1}{4} \lambda (\phi^\dagger \phi)^2\tag{1.31}$$

with the real parameters μ^2 and λ relating respectively to the mass term and the strength of the self-interaction. There are two sensible ranges for these parameters, depicted in Figure 1.2, the first one is the case $\lambda, \mu^2 > 0$, similar to the previous theories and only one solution in the minimisation. The second one is for $\lambda > 0$ and $\mu^2 < 0$, where the $\mu^2 \phi^\dagger \phi$ term cannot be understood as a mass term and the solution $\phi = 0$ is a local maximum, physically unstable. The minimum of the potential is degenerate and identified by the complex plane circle, $\phi^\dagger \phi = v^2/2$ with $v^2 \equiv -\mu^2/\lambda$ and

$$\phi = v e^{-i\theta}\tag{1.32}$$

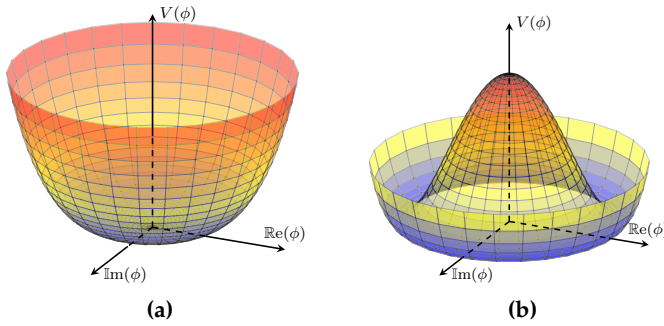


Figure 1.2: Shape of the potential $V(\phi)$ for $\lambda > 0$ and (a) $\mu^2 > 0$ or (b) $\mu^2 < 0$.

The symmetry is broken spontaneously when the system chooses the fundamental state. Suppose $\phi = 0$, then the *Vacuum Expectation Value* (VEV) of ϕ is set to,

$$\langle 0 | \phi | 0 \rangle = \frac{v}{\sqrt{2}}\tag{1.33}$$

Next, let's suppose the following change of variables to center the new fundamental state,

$$\phi(x) = \left(\frac{v + \eta(x)}{\sqrt{2}} \right) e^{i\zeta(x)/v} \quad (1.34)$$

the Lagrangian can be expressed as,

$$\begin{aligned} \mathcal{L} = & \frac{1}{2}(\partial_\mu \eta)^2 + \frac{1}{2}(\partial_\mu \zeta)^2 - \frac{1}{4}F_{\mu\nu}F^{\mu\nu} \\ & + \mu^2 \eta^2 + \frac{1}{2}g^2 v^2 A_\mu A^\mu - gv A_\mu \partial^\mu \zeta + \text{interactions} \end{aligned} \quad (1.35)$$

which now contains the η and ζ fields, additional to the gauge A_μ . Also, square terms appear for η and A_μ , which can be identified as mass terms, $\frac{m_\eta}{2}\eta^2$ and $\frac{m_A}{2}A_\mu A^\mu$, resulting in $m_\eta = \sqrt{-2\mu^2}$ and $m_A = gv$. $\zeta(x)$ is massless and a particular resulting type of field named *Goldstone boson*, which the *Goldstone theorem* predicts. The theorem states that a massless boson appears for every symmetry that the VEV spontaneously breaks. In this abelian case, the VEV is not invariant under the $U(1)$ transformation. $\zeta(x)$ does not appear explicitly in the potential, therefore can take any value without affecting the energy of the system, which is not very physical. In addition, it appears in an estrange mixing term with A_μ , $-gv A_\mu \partial^\mu \zeta$. A way to remove this annoyance is to choose the gauge,

$$\begin{aligned} \phi & \rightarrow \phi' = e^{-i\zeta/v} \phi \\ A_\mu & \rightarrow A'_\mu = A_\mu - \frac{1}{gv} \partial_\mu \zeta \end{aligned} \quad (1.36)$$

together with the previous change of variable for ϕ . Essentially the gauge freedom of the Lagrangian is being used to remove ζ , which becomes the longitudinal component of the transformed gauge boson A_μ . The gauge chosen is the so-called *unitary gauge*, which makes the physical content of the Lagrangian explicit⁶.

In summary, this process of acquiring mass by means of absorbing a Goldstone boson is known as the *Higgs mechanism*.

The Higgs-Englert-Brout Mechanism in the Electroweak Sector

The Higgs-Englert-Brout mechanism [25–27] solved the contradictions found between massive particles and the requirement of gauge invariance. The mechanism is based in a spontaneous symmetry breaking of the $SU(2)_L \otimes U(1)_Y$ to $U(1)_{EM}$, giving mass to the different particles involved in the EW interactions except the photon. A similar procedure can be applied to the EW Lagrangian derived in Equation 1.29, first introducing an isospin doublet ($Y=+1/2$) of complex scalar fields Φ , the Higgs field,

⁶ As a parallel, the ghost gluons in the context of regularisation also remove the problematic unphysical degrees of freedom.

$$\Phi \equiv \begin{pmatrix} \phi^+ \\ \phi^0 \end{pmatrix} = \frac{1}{\sqrt{2}} \begin{pmatrix} \phi_1 + i\phi_2 \\ \phi_3 + i\phi_4 \end{pmatrix} \quad (1.37)$$

where ϕ^+ corresponds to an electrically charged field ($T_3=+1/2$) and ϕ^0 to a neutral one ($T_3=-1/2$). This field transforms under $SU(2)_L$ and its Lagrangian, the Higgs Lagrangian,

$$\mathcal{L}_\Phi = (D_\mu \Phi)^\dagger (D^\mu \Phi) - V(\Phi) \quad (1.38)$$

with the same covariant derivative as in Equation 1.29 and the Higgs potential given by,

$$V(\Phi) = \mu^2 \Phi^\dagger \Phi + \lambda (\Phi^\dagger \Phi)^2 \quad (1.39)$$

which shape depends on the parameters μ^2 and λ . As seen before, choosing the case where $\lambda > 0$ and $\mu^2 < 0$, the potential at $\Phi = 0$ is unstable and a continuous collection of possible minimum values appear, defined by the circle,

$$\Phi^\dagger \Phi = \frac{1 - \mu^2}{2\lambda} \equiv \frac{1}{2}v^2 \quad (1.40)$$

Following, the spontaneous symmetry breaking with the choice of the new vacuum state,

$$\langle 0 | \Phi | 0 \rangle = \frac{1}{\sqrt{2}} \begin{pmatrix} 0 \\ v \end{pmatrix} \quad (1.41)$$

This vacuum is not invariant to any of the $SU(2)_L$ and the $U(1)$ transformations, however, the $Q = T_3 + Y$ transformation is not affected,

$$Q \langle 0 | \Phi | 0 \rangle = \frac{1}{2\sqrt{2}} \sigma_3 \begin{pmatrix} 0 \\ v \end{pmatrix} + \frac{1}{2\sqrt{2}} Y \begin{pmatrix} 0 \\ v \end{pmatrix} = \frac{1}{2\sqrt{2}} \left[\begin{pmatrix} 0 \\ -v \end{pmatrix} + \begin{pmatrix} 0 \\ v \end{pmatrix} \right] = \begin{pmatrix} 0 \\ 0 \end{pmatrix} \quad (1.42)$$

The field is rewritten in the unitary gauge, which automatically removes the extra nonphysical Goldstone bosons,

$$\Phi(x) = \frac{1}{\sqrt{2}} \begin{pmatrix} 0 \\ v + H(x) \end{pmatrix} \quad (1.43)$$

where $H(x)$ is centered around the vacuum state. With this change the Higgs potential becomes,

$$V(\Phi) = \frac{1}{4}\lambda v^2 H^2 + \frac{1}{4}\lambda v H^3 + \frac{1}{16}\lambda H^4 \quad (1.44)$$

spawning the Higgs boson mass $m_H^2 = \lambda v^2/2 = -\mu^2/2$, in the quadratic H term. The cubic and quartic terms constitute the three- and four-point Higgs boson self-interactions.

The EWSB generates new interactions and mass terms for the different particles involved in the EW interactions. Gluons are not affected as the scalar field is a doublet and does not transform under $SU(3)$. The effects on the boson and fermion sectors of the SM are discussed in the following, individually.

Boson sector

The gauge boson masses spawn from the covariant derivative, $(D_\mu \Phi)^\dagger (D^\mu \Phi)$, which includes the gauge fields. Expanding,

$$\mathcal{L}_{mass} = \frac{v^2}{8} V_\mu \begin{pmatrix} g^2 & 0 & & \\ 0 & g^2 & & \\ & & 0_{2 \times 2} & \\ 0_{2 \times 2} & & g^2 & -gg' \\ & & -gg' & g'^2 \end{pmatrix} V^\mu \quad (1.45)$$

with $V_\mu = (W_\mu^1 \ W_\mu^2 \ W_\mu^3 \ B_\mu)$. Diagonalising the matrix, the next eigenvectors are found,

$$\begin{aligned} A_\mu &\equiv \sin \theta_W W_\mu^3 + \cos \theta_W B_\mu \\ Z_\mu &\equiv \cos \theta_W W_\mu^3 - \sin \theta_W B_\mu \end{aligned} \quad (1.46)$$

where the Weinberg angle, or weak mixing angle, is defined by $\tan \theta_W \equiv g'/g$. The corresponding eigenvalues, the square masses, for the A_μ and Z_μ fields are zero and $v^2(g^2 + g'^2)/8$. On the other side, W_μ^1 and W_μ^2 are well defined mass states but not charge states. This is due T_1 and T_2 being not diagonal, connecting the different states of T_3 (hence of Q). The operator $T_\pm = T_1 \mp iT_2$ can be defined, which increases or decreases one unit of T_3 (hence of Q). In addition, the fields can be redefined,

$$W_\mu^\pm = \frac{1}{\sqrt{2}} (W_\mu^1 \mp iW_\mu^2) \quad (1.47)$$

In summary the Lagrangian in Equation 1.45 can now be written as

$$\mathcal{L}_{mass} = \frac{g^2 v^2}{4} W_\mu^+ W^{-\mu} - \frac{v^2}{8} (g^2 + g'^2) Z_\mu Z^\mu \quad (1.48)$$

where the mass terms of the different bosons can be identified,

$$\begin{aligned}
m_A &= 0 \\
m_Z &= \frac{v}{2} \sqrt{g^2 + g'^2} \\
m_W &= \frac{vg}{2} = m_Z \cos \theta_W
\end{aligned} \tag{1.49}$$

Note that the remaining symmetry after breaking $SU(2)_L \otimes U(1)_L$ is $U(1)_{EM}$. The associated A_μ field is massless, the photon, which is a combination of the W_μ^3 and B_μ fields. The associated quantum number, the electric charge, has been defined previously in the chapter, $Q = T_3 - Y$.

Regarding interactions, the covariant derivative can be expressed in terms of the new bosons,

$$\partial_\mu - igW_\mu^3 = \partial_\mu - ig \sin \theta_W A_\mu - ig \cos \theta_W Z_\mu \tag{1.50}$$

where the electromagnetic coupling constant e can be defined as $e = g \sin \theta_W$. In addition, the field tensors can be rewritten as,

$$\begin{aligned}
W_{\mu\nu}^3 &= \partial_\mu W_\nu^3 - \partial_\nu W_\mu^3 - ig(W_\mu^+ W_\nu^- - W_\nu^+ W_\mu^-) \\
&= \sin \theta_W F_{\mu\nu} + \cos \theta_W Z_{\mu\nu} - ig(W_\mu^+ W_\nu^- - W_\nu^+ W_\mu^-) \\
B_{\mu\nu} &= \cos \theta_W F_{\mu\nu} - \sin \theta_W Z_{\mu\nu}
\end{aligned} \tag{1.51}$$

where the field strength tensors for the photons and the Z boson, $F_{\mu\nu}$ and $Z_{\mu\nu}$ are defined.

Fermion sector

The procedure required to acquire the fermion masses is more complicated than for the gauge bosons. Instead of just expanding the kinematic term with the new Higgs field, Yukawa [28] interactions that couple left- and right-handed fermions with the Higgs need to be introduced.

As seen in this chapter, only $q_{\alpha L}^i$ and l_L^i fields are $SU(2)_L$ doublets,

$$q_{\alpha L}^i = \begin{pmatrix} u_{\alpha L}^i \\ d_{\alpha L}^i \end{pmatrix}, \quad l_L^i = \begin{pmatrix} \nu_L^i \\ \ell_L^i \end{pmatrix} \tag{1.52}$$

where the i refers to the generation and α to the colour. It has been already pointed out that is not possible to construct a well defined $mf^\dagger f$ term that transforms under the SM group, necessary for gauge invariance.

The solution is provided by introducing Yukawa interactions between the fermion fields and the Higgs field Φ , also a doublet under $SU(2)$,

$$\mathcal{L}_{Yukawa} = -y^{ab}\bar{q}_{\alpha L}^a \Phi d_{\alpha R}^b - y'^{ab}\bar{q}_{\alpha L}^a \tilde{\Phi} u_{\alpha R}^b - y''^{ab}\bar{l}_L^a \Phi \ell_R^b + \text{h.c} \quad (1.53)$$

where y , y' and y'' are the Yukawa matrices, 3×3 matrices with one dimension for each generation. Also, $\tilde{\Phi} \equiv i\sigma_2 \Phi^*$. Note that there is no second term for the leptons, as the SM does not contemplate the right handed neutrino, ν_R . Also, this Lagrangian breaks explicitly the chiral symmetry but yields a singlet representation, safe for gauge invariance. Next, writing the field Φ in terms of the unitary gauge as in the EWSB, $\phi^0(x) = v + H(x)$,

$$\begin{aligned} \mathcal{L}_{Yukawa} &= -\frac{1}{\sqrt{2}}(v + H)y^{ab}\bar{q}_{\alpha L}^a d_{\alpha R}^b - \frac{1}{\sqrt{2}}(v + H)y'^{ab}\bar{q}_{\alpha L}^a u_{\alpha R}^b \\ &\quad - \frac{1}{\sqrt{2}}(v + H)y''^{ab}\bar{l}_L^a \ell_R^b + \text{h.c} \\ &= -\frac{1}{\sqrt{2}}(v + H)y^{ab}\bar{D}_{\alpha}^a D_{\alpha}^b - \frac{1}{\sqrt{2}}(v + H)y'^{ab}\bar{U}_{\alpha}^a U_{\alpha}^b \\ &\quad - \frac{1}{\sqrt{2}}(v + H)y''^{ab}\bar{L}^a L^b + \text{h.c} \end{aligned} \quad (1.54)$$

where the expression has been rearranged to define Dirac fields in spinor notation,

$$D_{\alpha}^a = \begin{pmatrix} d_{\alpha}^a \\ \bar{d}_{\alpha}^{+a} \end{pmatrix}, \quad U_{\alpha}^a = \begin{pmatrix} u_{\alpha}^a \\ \bar{u}_{\alpha}^{+a} \end{pmatrix}, \quad L_{\alpha}^a = \begin{pmatrix} \ell_{\alpha}^a \\ \bar{\ell}_{\alpha}^{+a} \end{pmatrix} \quad (1.55)$$

After diagonalising the three Yukawa matrices, the eigenvalues terms are related to the masses, which can be identified for each generation as,

$$\begin{aligned} m_{d^i} &= y^{ii}v/\sqrt{2} \\ m_{u^i} &= y'^{ii}v/\sqrt{2} \\ m_{\ell^i} &= y''^{ii}v/\sqrt{2} \\ m_{\nu^i} &= 0 \end{aligned} \quad (1.56)$$

There is a major consequence from the differences between the representation in generation space (Equation 1.52, $SU(2)_L$ doublets), and in mass space, after diagonalising the Yukawa matrices. D_{α}^a and U_{α}^a are rotated to diagonalise their corresponding Yukawa matrix, so affected by different transformations. However, the individual $d_{\alpha L}^a$ and $u_{\alpha L}^a$ fields are part of the same $SU(2)_L$ doublet. The effect can be seen writing the W^{\pm} interactions in the mass state representation of the fields which become off-diagonal,

$$\frac{-g}{\sqrt{2}} \begin{pmatrix} \bar{u}_L & \bar{c}_L & \bar{t}_L \end{pmatrix} \gamma^\mu W_\mu^+ V_{CKM} \begin{pmatrix} d_L \\ s_L \\ b_L \end{pmatrix} + \text{h.c} \quad (1.57)$$

$$\begin{pmatrix} d'_L \\ s'_L \\ b'_L \end{pmatrix} = V_{CKM} \begin{pmatrix} d_L \\ s_L \\ b_L \end{pmatrix} = \begin{pmatrix} V_{ud} & V_{us} & V_{ub} \\ V_{cd} & V_{cs} & V_{cb} \\ V_{td} & V_{ts} & V_{tb} \end{pmatrix} \begin{pmatrix} d_L \\ s_L \\ b_L \end{pmatrix} \quad (1.58)$$

where the superscript ' denotes the mass representation and V_{CKM} is the Cabibbo-Kobayashi-Maskawa matrix [29, 30]. This unitary matrix is the product of the transformations that diagonalise the y and y' Yukawa matrices, which encodes the mixing of the different generations of fields in charged-mediated weak interactions. This is known as flavour violation, where a weak interaction of a quark can result on changing its flavour. On the other side, leptons are represented with the same $SU(2)_L$ doublet, so any mixing of lepton generations is not present in the theory.

feynman diagram?

There is still another interesting feature that arises from the CKM matrix. The standard representation [31] of the matrix takes into account invariant phase rotations of the fields, leaving as free parameters three angles θ_{12} , θ_{23} and θ_{13} (chosen to lie in the first quadrant so $\sin \theta, \cos \theta \geq 0$), and a single complex phase δ that cannot be rotated to zero. The matrix reads,

$$\begin{aligned} V_{CKM} &= \begin{pmatrix} 1 & 0 & 0 \\ 0 & c_{23} & s_{23} \\ 0 & -s_{23} & c_{23} \end{pmatrix} \begin{pmatrix} c_{13} & 0 & s_{13}e^{-i\delta} \\ 0 & 1 & 0 \\ -s_{13}e^{i\delta} & 0 & c_{13} \end{pmatrix} \begin{pmatrix} c_{12} & s_{12} & 0 \\ -s_{12} & c_{12} & 0 \\ 0 & 0 & 1 \end{pmatrix} \\ &= \begin{pmatrix} c_{12}c_{13} & s_{12}c_{13} & s_{13}e^{-i\delta} \\ -s_{12}c_{23} - c_{12}s_{23}s_{13}e^{i\delta} & c_{12}c_{23} - s_{12}s_{23}s_{13}e^{i\delta} & s_{23}c_{13} \\ s_{12}s_{23} - c_{12}c_{23}s_{13}e^{i\delta} & -c_{12}s_{23} - s_{12}c_{23}s_{13}e^{i\delta} & c_{23}c_{13} \end{pmatrix} \end{aligned} \quad (1.59)$$

where $s_{ij} = \sin \theta_{ij}$ and $c_{ij} = \cos \theta_{ij}$. The presence of the complex phase leads to different couplings for anti-matter, as the complex phase will switch sign, thus leading to matter/anti-matter asymmetry. This asymmetry in flavour-changing processes is the only source in the SM of CP violation, or T violation (from the time-reversal symmetry⁷) however, as discussed in Section 1.2.4, fails to describe the current matter/anti-matter content of the universe. The CKM matrix is predicted and measured to be almost diagonal, with very small sources of CP violation, or V_{ub} and V_{td} . The current matrix as in 2022 [16] reads,

$$V_{CKM} = \begin{pmatrix} 0.97401 \pm 0.00011 & 0.22650 \pm 0.00048 & 0.00361^{+0.00011}_{-0.00009} \\ 0.22636 \pm 0.00048 & 0.97320 \pm 0.00011 & 0.04053^{+0.00083}_{-0.00061} \\ 0.00854^{+0.00023}_{-0.00016} & 0.03978^{+0.00082}_{-0.00060} & 0.999172^{+0.000024}_{-0.000035} \end{pmatrix} \quad (1.60)$$

⁷ The three symmetries are related as the combination, CPT symmetry, which must always be respected in theory.

1.1.6 Flavour Changing Neutral Currents interactions

Flavour Changing Neutral Currents (FCNC) are the processes that involve the change of a fermion flavour through a neutral boson. In the electroweak sector, the neutral current interactions are mediated by the Z boson. Contrary to the W^\pm case, the interactions involving the Z boson involve fields with the same associated Yukawa matrix, from the same spinors of the mass representation (Equation 1.55). Hence, no mixing matrix spawns thus are no explicit FCNC appear in the SM Lagrangian.

The existence of charged flavour changing currents is allowed at tree level but their associated couplings are proportional to the off-diagonal elements of the CKM matrix, which are specially small for the interactions between the first and third generation leptons. However, FCNC processes can be obtained from consecutive flavour changing interactions in higher order diagrams. Figure X shows two example FCNC processes involving the two types of first order Feynman diagrams, known as *box* and *penguin* diagrams.

The high-order contributions are suppressed further by the Glashow, Iliopoulos and Maiani (GIM) mechanism [32]. In order to illustrate this mechanism, the example penguin diagram is discussed in the following. The diagram depicts a top FCNC decay that involves the $t \rightarrow b$ and $b \rightarrow c$ type of interactions, thus the interaction will be proportional to $V_{cb}^* V_{tb}$. Adding up the other two possible diagrams with d and s in the loop,

$$V_{cd}^* V_{td} + V_{cs}^* V_{ts} + V_{cb}^* V_{tb} \quad (1.61)$$

which assumes that the quarks have the same mass. The value of this expression can be obtained from the CKM matrix. As the matrix is unitary ($V_{CKM} V_{CKM}^\dagger = V_{CKM}^\dagger V_{CKM} = 1$), a total of 18 constraints appear, relating the different vertices:

$$\begin{aligned} V_{ud}^2 + V_{cd}^2 + V_{td}^2 &= 1, & V_{ud}^2 + V_{us}^2 + V_{ub}^2 &= 1 \\ V_{us}^2 + V_{cs}^2 + V_{ts}^2 &= 1, & V_{cd}^2 + V_{cs}^2 + V_{cb}^2 &= 1 \\ V_{ub}^2 + V_{cb}^2 + V_{tb}^2 &= 1, & V_{td}^2 + V_{ts}^2 + V_{tb}^2 &= 1 \end{aligned}$$

$$\begin{aligned} V_{ud}^* V_{us} + V_{cd}^* V_{cs} + V_{td}^* V_{ts} &= 0, & V_{ud}^* V_{cd} + V_{us}^* V_{cs} + V_{ub}^* V_{cb} &= 0 \\ V_{ud}^* V_{ub} + V_{cd}^* V_{cb} + V_{td}^* V_{tb} &= 0, & V_{ud}^* V_{td} + V_{us}^* V_{ts} + V_{ub}^* V_{tb} &= 0 \\ V_{us}^* V_{ud} + V_{cs}^* V_{cd} + V_{ts}^* V_{td} &= 0, & V_{cd}^* V_{ud} + V_{cs}^* V_{us} + V_{cb}^* V_{ub} &= 0 \\ V_{us}^* V_{ub} + V_{cs}^* V_{cb} + V_{ts}^* V_{tb} &= 0, & V_{cd}^* V_{td} + V_{cs}^* V_{ts} + V_{cb}^* V_{tb} &= 0 \\ V_{ub}^* V_{ud} + V_{cb}^* V_{cd} + V_{tb}^* V_{td} &= 0, & V_{td}^* V_{ud} + V_{ts}^* V_{us} + V_{tb}^* V_{ub} &= 0 \\ V_{ub}^* V_{us} + V_{cb}^* V_{cs} + V_{tb}^* V_{ts} &= 0, & V_{td}^* V_{cd} + V_{ts}^* V_{cs} + V_{tb}^* V_{cb} &= 0 \end{aligned} \quad (1.62)$$

box K-
>ll and
t->c with
b and
vertices

The equation is exactly one of the constraints, and equals zero. However, as the different quarks are not degenerate in mass, every term would be proportional to $1/m_q$ (q being the quark inside the loop). This is the origin of the GIM mechanism and results in a non-zero but very suppressed contribution of FCNC in the SM. In addition, this suppression is larger for loops involving down-type quarks as their masses are more similar than for the up-type quarks.

1.2 Standard Model measurements and top physics

Since the formulation of the SM, most experimental observations and measurements have been described successfully by the model. Throughout the years, predicted particles have been found and multiple precision measurements have tested its validity. However, there are theoretical and experimental issues that are not solved, leading to the conclusion that the SM is an effective theory and there is a more complete theory that can explain the whole range of observations. In this section, a summary of the measurements of the SM is presented, focusing in processes involving the top quark and FCNC. Then, different main open questions of the SM are briefly reviewed.

1.2.1 Experimental measurements

Decades of experiments have performed measurements into parameters that define the SM. The SM can be summarised with nineteen parameters, which have been described in this chapter: nine fermion masses (six for quarks, three for leptons), the three gauge couplings (g_s , g and g'), the Higgs vacuum expectation value (v), the Higgs mass, four parameters of the CKM matrix (three angles and the complex phase) and the QCD CP violating phase. There is no underlying relation between these parameters, only being set from experimental observations. With these parameters measured, theoretical predictions of observables can be tested with experimental data in order to explore new physics.

One typical observable in particle physics is the cross-section σ , the expected interaction rate between two interacting particles in terms of the effective surface area typically measured in pb (picobarn, $1pb = 10^{-40} \text{ m}^2$). The cross-section of a process depends on the interacting forces involved, as well as the energy and momentum of the interacting particles, which can be calculated from the S-matrix (scattering matrix) using relativistic mechanics. Feynman diagrams are a tool to translate a visual description of a process to a mathematical expression, the matrix amplitude, which is proportional to the probability of the specific process happening and needed for the computation. The decay width, Γ , can be computed in similar fashion to obtain another common observable, the Branching Ratio (BR). The BR of an unstable particle is the probability for it to decay into specific particles among all possible states. It is computed dividing the Γ of the specific process with respect to the sum of all the possible process. Both σ and Γ are calculated from perturbation approximations, as the actual process is not the product of just one

Feynman diagram, but all the possible interactions that lead to the same final state including loops, interferences and radiative corrections, referred to as high order corrections. However, each particle interaction is proportional to the probability making higher order corrections become less important. Typically, *leading-order* (LO) calculations use only the leading order terms from the perturbation expansion, while if complemented by higher order corrections are referred to next-to-leading-order (NLO) or next-to-NLO (NNLO) calculations.

Figure 1.3 shows a summary of a wide range of cross-section measurements by the ATLAS Collaboration, compared to the theoretical predictions, showing an excellent agreement between data and theory. In addition, the Higgs boson has been scrutinised since its discovery, to characterise all its properties, unique for its interaction with massive particles. Figure 1.4 shows a summary of Higgs boson production cross-sections and branching ratios by the ATLAS collaboration, including the coupling strengths to other SM particles, showing that the coupling is proportional with the mass of the resulting particle as expected from the Higgs mechanism. As the Higgs couples with any particle that acquires mass through its field, it is an excellent candidate to study any other particle still to be discovered.

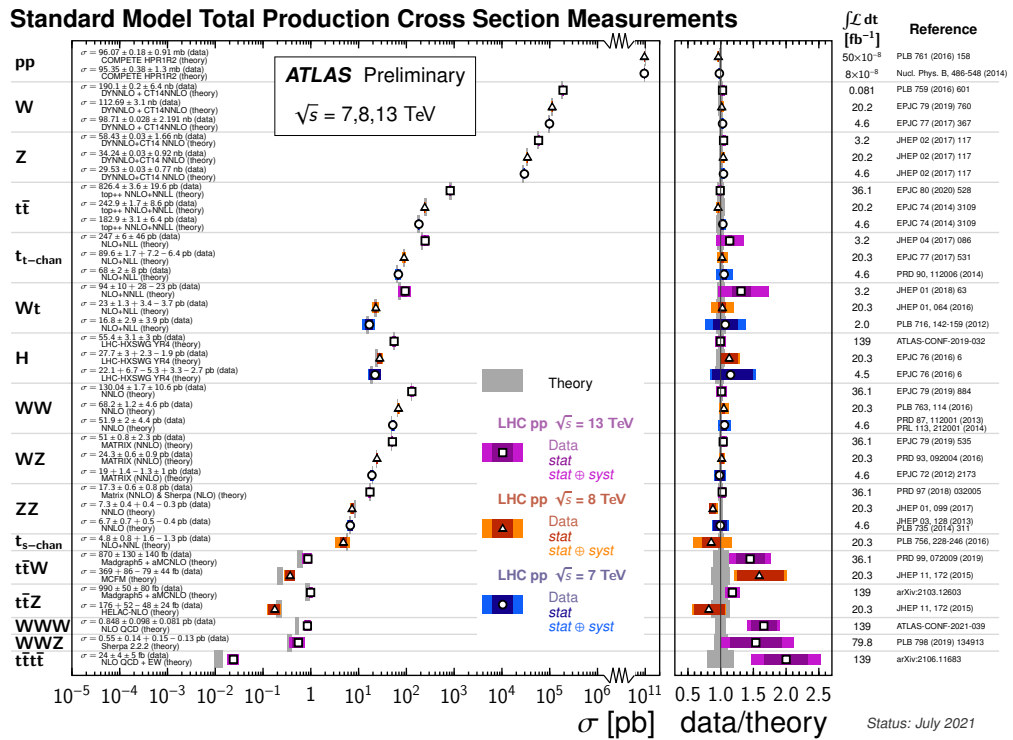


Figure 1.3: Summary of several SM total production cross-section measurements, corrected for branching fractions, compared to the corresponding theoretical predictions and ratio with respect to theory [33].

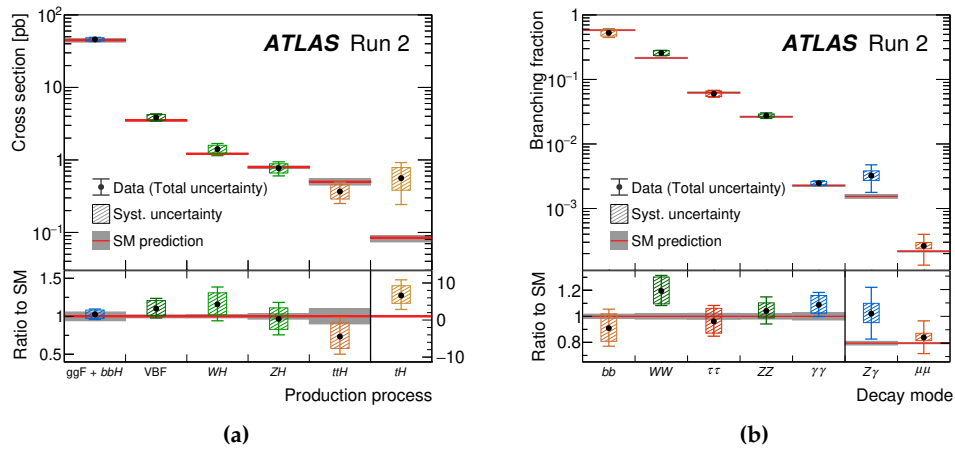


Figure 1.4: Observed and predicted Higgs boson production cross-sections for different production processes (a) and for different decay modes (b). The lower panels show the ratios of the measured values to their SM predictions. The vertical bar on each point denotes the 68% confidence interval. The p-value for compatibility of the measurement and the SM prediction is 65% (a) or 56% (b) [34].

1.2.2 Top quark physics

The top quark is the most massive known elementary particle, discovered in 1995 at Fermilab [11, 12]. Such characteristic makes the top quark the only one that decays before hadronisation and hence, properties like the spin are directly transferred to the decay products. The main top quark decay is $t \rightarrow Wb$ with a branching ratio close to 1, determined by the $V_{tb} = 0.97401 \pm 0.00011$ (element of the CKM matrix [16]) being very close to 1. Due to its higgs mass, the top quark strongly couples with the Higgs boson as the Yukawa coupling (Equation 1.56) $y_t = \sqrt{2}m_t/v \simeq 1$.

Altogether, the top quark plays a key role in the study of the SM. The precise measurements of its properties put the theory to test and any deviation would point to new physics. It is also an excellent candidate for searches involving either much more massive particles that might decay to the top quark, or decay into other lighter exotic particles. Even if those new particles are too heavy to be produced at the LHC, they can be targetted by indirect searches and modify the top quark properties.

The top quark can be produced either in top quark pairs, namely $t\bar{t}$ production, or together with other particles, called single-top production. The $t\bar{t}$ production is mainly involves the strong interaction and the main Feynman diagrams are shown in Figure

The single-top production has three different channels, which involve electroweak interactions: t -channel, from W /gluon fusion; Wt -channel, with an associated W ; and s -channel, from $q\bar{q}' \rightarrow tb$. Example Feynman diagrams are shown in Figure

Figure 1.5 shows a comparison of theoretical and experimental values for the different cross-sections involving the production of different top processes, showing an excellent agreement between them. Also, that the $t\bar{t}$ production is larger than the single-top.

qq->t \bar{t} bar,
gg->t \bar{t} bar,
crossed,
s-channel

qb->q't
tchannel,
gb->tW
Wt, qq'-
>tb

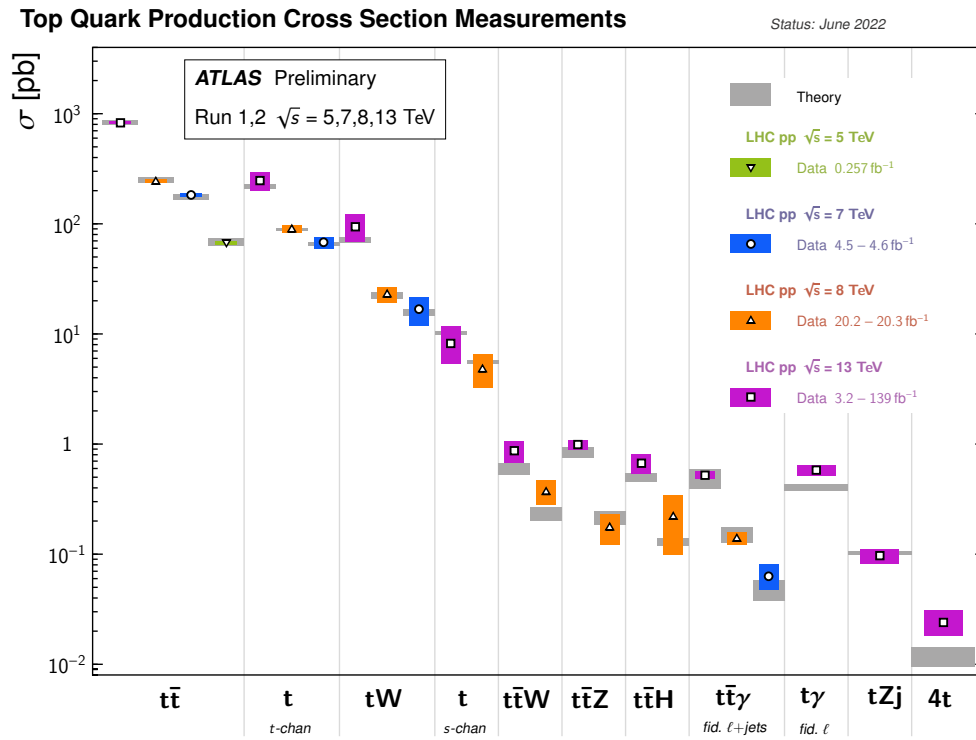


Figure 1.5: Summary of several top-quark related production cross-section measurements, compared to the corresponding theoretical expectations. All theoretical expectations were calculated at NLO or higher [35].

1.2.3 FCNC measurements

A FCNC process stands for an interaction with a change in the fermion (quark or lepton) flavour through the emission or absorption of a neutral boson. As seen in Section 1.1.6, such processes are not allowed at tree-level in the SM and the one-loop contributions are heavily suppressed by the GIM mechanism.

The FCNC interactions involving the top quark are of particular interest, and the possible diagrams are depicted in Figure. As the branching ratio of the top quark is mainly $t \rightarrow Wb$, together with the heavily suppressed FCNC contributions, the predicted branching ratio for the top FCNC decays in the SM is below 10^{-14} . This very small value is far away from the achievable sensitivity at the LHC, and makes the precise measurement of FCNC interactions an excellent test of the SM.

depict
tgamam
uc, tZ uc,
tglu uc,
tH uc

Table 1.3 shows the SM predictions for all the FCNC top quark decays, together with the experimental results from the SM and CMS collaborations.

Table 1.3: Theoretical predictions for the branching ratios of FCNC top decays predicted with the SM and the most recent experimental limits from the ATLAS and the CMS collaborations.

Process	SM	ATLAS	CMS
$t \rightarrow u\gamma$	$4 \cdot 10^{-16}$	number ref	number ref
$t \rightarrow c\gamma$	$5 \cdot 10^{-14}$	number ref	number ref
$t \rightarrow ug$	$4 \cdot 10^{-14}$	number ref	number ref
$t \rightarrow cg$	$5 \cdot 10^{-12}$	number ref	number ref
$t \rightarrow uZ$	$7 \cdot 10^{-17}$	number ref	number ref
$t \rightarrow cZ$	$1 \cdot 10^{-14}$	number ref	number ref
$t \rightarrow uH$	$2 \cdot 10^{-17}$	number ref	number ref
$t \rightarrow cH$	$3 \cdot 10^{-15}$	number ref	number ref

1.2.4 Open questions

Observed neutrino oscillations [36] are only possible if there are mass differences between the three neutrino generations, which implies non-zero masses for some neutrinos although not directly measured. A mass term for neutrinos could be added in the SM in different ways, through adding right-handed neutrinos or as describing neutrinos as Majorana particles [ref]. Nevertheless, the description of the SM particles needs at least seven additional parameters: three for the neutrino masses, three for their mixing angles and one CP violating phase for the neutrino mixing Pontecorvo-Maki-Nakagawa-Sakata (PMNS) matrix [], similar to the CKM quark flavor matrix.

Other measurements that are in tension with the SM predictions are regarding the lepton universality, which is the prediction that charged leptons have identical electroweak interaction strenghts. However, the LHCb collaboration found in 2021 [3] a discrepancy between electrons and muons in decays involving the b -quark. An

older puzzle is the measurement of the anomalous magnetic dipole momentum of the muon, which was found also in tension with the prediction. This quantity refers to the high order corrections that appear from QCD, and the muon g-2 experiment found a greater deviation [4] in 2021.

The SM also fails to describe the other known fundamental force in nature, gravity. There is no renormalisable QFT for gravity successfully described as general relativity only describes macroscopic systems, with the observation of gravitational waves as a recent achievement[]. There are theories like string theory that provide alternatives although difficult to test experimentally. The SM is understood as an effective theory of a more complete unified theory, hence only valid at low energies and it is expected to break in the most extreme scenario around the Plank scale ($M_P = \sqrt{\hbar/(8\pi G_N)} \sim 2.4 \cdot 10^{18}$ GeV), where gravitational effects are expected to become as important as the other forces in the SM.

The SM describes what is known as baryonic matter, which accounts for about 5% of the energy density of the universe. Cosmology, which studies the composition of the universe, estimates huge amounts of *dark matter* (DM) and *dark energy*, phenomena not contemplated by the SM. The existence of DM was postulated as extra non-luminous matter needed to explain observed rotation curves of galaxies not matching the gravitational pull of observed stars[]. In addition, gravitational lensing effects observed in some galaxy collisions[] also provide the need of huge invisible mass concretations. More recently, the WMAP and Planck collaborations have studied anisotropies in the cosmic microwave background (CMB)[], postulating cold DM. On the other side, the universe is observed to be expanding at an accelerated rate compatible with dark energy, understood to be the product of an intrinsic space-time energy density, or cosmological constant, that causes the expansion. Observation of red-shift of light from supernovae, used as standard candles, points that cosmological objects are moving away at faster rate with the distance[]. Further, studies of the CMB provide another measurements of the accelerated expansion[]. The most updated results[] points that baryonic matter accounts for a mere % of the total energy density of the universe, dark matter for %, while dark energy for %.

The universe seems to be completely made up by matter. To explain the imbalance in abundance of matter and anti-matter, often referred as matter/anti-matter assymetry, the SM only provides one not nearly sufficient source of CP violation in the quark weak interactions. Additional sources are added such as the complex phase in the PMNS matrix, however more phenomena is needed to have generated the current net balance of matter, like possible baryon number violating effects at high energy scales.

Besides the natural phenomena uncovered by the SM, there are also what are known as naturalness problems. Those are aesthetic concerns about the precise different values of some of the SM parameters, which seem "unnatural" if there is no hidden mechanism behind. The general consensus is that the fewer fine tuning is needed in a theory, the more natural it is. Although these matters are completely subjective, these unexplained features could be a hint for the existence of a new underlying mechanism that could complement the SM. The first problem is commonly named as

the hierarchy problem, where the cutoff energy of the SM (Λ_{SM}) is commonly set to the Planck scale, $\sim 10^{18}$ GeV, but in contrast the EW scale ($v \sim 246$ GeV) is very small. The problem can be read as there is no apparent reason for the EWSB to happen at its scale, orders of magnitude smaller than the Plank scale. When calculating high-order corrections from the SM, one obtains that the leading radiation corrections for the fermion masses are of the order of $\log \Lambda_{\text{SM}}$, sensitive to the scale but the fine-tuning is considered small. On the other side, the physical Higgs mass including radiation corrections reads,

$$m_H^2 = m_0^2 + \frac{3}{8\pi^2 v^2} \Lambda_{\text{SM}}^2 [m_0^2 + 2m_W^2 + M_Z^2 - 4m_t^2] + \mathcal{O}(\ln \frac{\Lambda_{\text{SM}}}{m_0}) \quad (1.63)$$

with m_0 the bare Higgs mass. The nature of the hierarchy problem is evident in the correction as the Higgs mass is more sensitive to the cutoff scale and requires huge tuning to counter the Λ_{SM} term and achieve such a low measured physical mass. It can also be observed that the most important correction is given by the top quark, and it is often questioned whether the reason for the huge mass of this quark could hide a solution. Although the Higgs mass and the EW scale are difficult to justify, it can be argued that the appearance of the Λ_{SM} is related to the chosen regularisation scheme and cut-offs play no physical role.

Another related problem is the fermion mass hierarchy, as the fact that the masses of the SM particles range from ~ 1 MeV to ~ 173 GeV (of the top quark [16]), it is not understood. Additionally, there is also not an apparent reason for the three mass families of quarks and leptons. It might be related again to renormalisation, since fermion masses also have correction terms with the logarithm of the cut-off scale as stated before.

There is also the problem known as the strong CP problem. The most general QCD Lagrangian could include a CP-violating angle without breaking any symmetry or the renormalisability of the theory. This would lead to the prediction of axion particles and the neutron having non-zero electric dipole moment. Measures of the former in ultracold neutrons and mercury, constrain the CP-violating angle to $|\theta| \lesssim 10^{-10}$ [1], and supposes an incredibly low value for a parameter that can have any value in the theory.

The ATLAS experiment at the LHC

2

CHARGED HIGGS BOSON WITH $H^\pm \rightarrow tb$
SEARCH

**NEUTRAL SCALAR PRODUCED IN $t \rightarrow qX$
WITH $X \rightarrow b\bar{b}$ SEARCH**

APPENDIX

Bibliography

Here are the references in citation order.

- [1] G. Aad et al. ‘Observation of a new particle in the search for the Standard Model Higgs boson with the ATLAS detector at the LHC’. In: *Physics Letters B* 716.1 (2012), 1–29. doi: [10.1016/j.physletb.2012.08.020](https://doi.org/10.1016/j.physletb.2012.08.020) (cited on pages 1, 5).
- [2] S. Chatrchyan et al. ‘Observation of a new boson at a mass of 125 GeV with the CMS experiment at the LHC’. In: *Physics Letters B* 716.1 (2012), 30–61. doi: [10.1016/j.physletb.2012.08.021](https://doi.org/10.1016/j.physletb.2012.08.021) (cited on pages 1, 5).
- [3] LHCb Collaboration et al. *Test of lepton universality in beauty-quark decays*. 2021. doi: [10.48550/ARXIV.2103.11769](https://doi.org/10.48550/ARXIV.2103.11769). URL: <https://arxiv.org/abs/2103.11769> (cited on pages 1, 30).
- [4] B. Abi et al. ‘Measurement of the Positive Muon Anomalous Magnetic Moment to 0.46 ppm’. In: *Phys. Rev. Lett.* 126 (14 2021), p. 141801. doi: [10.1103/PhysRevLett.126.141801](https://doi.org/10.1103/PhysRevLett.126.141801) (cited on pages 1, 31).
- [5] and M. Aaboud, G. Aad, and B. Abbott. ‘Search for charged Higgs bosons decaying into top and bottom quarks at $\sqrt{s}=13$ TeV with the ATLAS detector’. In: *Journal of High Energy Physics* 2018.11 (2018). doi: [10.1007/jhep11\(2018\)085](https://doi.org/10.1007/jhep11(2018)085) (cited on page 1).
- [6] ATLAS Collaboration. *Search for flavour-changing neutral current interactions of the top quark and the Higgs boson in events with a pair of τ -leptons in pp collisions at $\sqrt{s} = 13$ TeV with the ATLAS detector*. ATLAS-CONF-2022-014. 2022 (cited on page 2).
- [7] Armen Tumasyan et al. ‘Search for flavor-changing neutral current interactions of the top quark and the Higgs boson decaying to a bottom quark-antiquark pair at $\sqrt{s} = 13$ TeV’. In: *JHEP* 02 (2022), p. 169. doi: [10.1007/JHEP02\(2022\)169](https://doi.org/10.1007/JHEP02(2022)169) (cited on page 2).
- [8] Steven Weinberg. ‘A Model of Leptons’. In: *Phys. Rev. Lett.* 19 (21 1967), pp. 1264–1266. doi: [10.1103/PhysRevLett.19.1264](https://doi.org/10.1103/PhysRevLett.19.1264) (cited on page 5).
- [9] Sheldon L. Glashow. ‘Partial-symmetries of weak interactions’. In: *Nuclear Physics* 22.4 (1961), pp. 579–588. doi: [https://doi.org/10.1016/0029-5582\(61\)90469-2](https://doi.org/10.1016/0029-5582(61)90469-2) (cited on page 5).
- [10] Abdus Salam. ‘Gauge unification of fundamental forces’. In: *Rev. Mod. Phys.* 52 (3 1980), pp. 525–538. doi: [10.1103/RevModPhys.52.525](https://doi.org/10.1103/RevModPhys.52.525) (cited on page 5).
- [11] S. Abachi et al. ‘Search for High Mass Top Quark Production in pp Collisions at $\sqrt{s}=1.8$ TeV’. In: *Physical Review Letters* 74.13 (1995), 2422–2426. doi: [10.1103/physrevlett.74.2422](https://doi.org/10.1103/physrevlett.74.2422) (cited on pages 5, 28).
- [12] ‘Observation of Top Quark Production in $\bar{p}p$ Collisions with the Collider Detector at Fermilab’. In: *Phys. Rev. Lett.* 74 (14 1995), pp. 2626–2631. doi: [10.1103/PhysRevLett.74.2626](https://doi.org/10.1103/PhysRevLett.74.2626) (cited on pages 5, 28).
- [13] H. Fritzsch, M. Gell-Mann, and H. Leutwyler. ‘Advantages of the color octet gluon picture’. In: *Physics Letters B* 47.4 (1973), pp. 365–368. doi: [https://doi.org/10.1016/0370-2693\(73\)90625-4](https://doi.org/10.1016/0370-2693(73)90625-4) (cited on page 5).
- [14] Abdus Salam. ‘Weak and Electromagnetic Interactions’. In: *Conf. Proc. C* 680519 (1968), pp. 367–377. doi: [10.1142/9789812795915_0034](https://doi.org/10.1142/9789812795915_0034) (cited on page 5).

- [15] W. Pauli. 'Über den Zusammenhang des Abschlusses der Elektronengruppen im Atom mit der Komplexstruktur der Spektren'. In: *Zeitschrift für Physik* 31.1 (1925), pp. 765–783. doi: [10.1007/BF02980631](https://doi.org/10.1007/BF02980631) (cited on page 6).
- [16] P.A. Zyla et al. 'Review of Particle Physics'. In: *PTEP* 2020.8 (2020), p. 083C01. doi: [10.1093/ptep/ptaa104](https://doi.org/10.1093/ptep/ptaa104) (cited on pages 6, 7, 23, 28, 32).
- [17] Emmy Noether. 'Invariant variation problems'. In: *Transport Theory and Statistical Physics* 1.3 (1971), pp. 186–207. doi: [10.1080/00411457108231446](https://doi.org/10.1080/00411457108231446) (cited on page 8).
- [18] C. N. Yang and R. L. Mills. 'Conservation of Isotopic Spin and Isotopic Gauge Invariance'. In: *Phys. Rev.* 96 (1 1954), pp. 191–195. doi: [10.1103/PhysRev.96.191](https://doi.org/10.1103/PhysRev.96.191) (cited on page 9).
- [19] Murray Gell-Mann. 'Symmetries of Baryons and Mesons'. In: *Phys. Rev.* 125 (3 1962), pp. 1067–1084. doi: [10.1103/PhysRev.125.1067](https://doi.org/10.1103/PhysRev.125.1067) (cited on page 11).
- [20] C. Abel et al. 'Measurement of the Permanent Electric Dipole Moment of the Neutron'. In: *Phys. Rev. Lett.* 124 (8 2020), p. 081803. doi: [10.1103/PhysRevLett.124.081803](https://doi.org/10.1103/PhysRevLett.124.081803) (cited on page 12).
- [21] H. David Politzer. 'Reliable Perturbative Results for Strong Interactions?' In: *Phys. Rev. Lett.* 30 (26 1973), pp. 1346–1349. doi: [10.1103/PhysRevLett.30.1346](https://doi.org/10.1103/PhysRevLett.30.1346) (cited on page 12).
- [22] David J. Gross and Frank Wilczek. 'Ultraviolet Behavior of Non-Abelian Gauge Theories'. In: *Phys. Rev. Lett.* 30 (26 1973), pp. 1343–1346. doi: [10.1103/PhysRevLett.30.1343](https://doi.org/10.1103/PhysRevLett.30.1343) (cited on page 12).
- [23] T. D. Lee and C. N. Yang. 'Question of Parity Conservation in Weak Interactions'. In: *Phys. Rev.* 104 (1 1956), pp. 254–258. doi: [10.1103/PhysRev.104.254](https://doi.org/10.1103/PhysRev.104.254) (cited on page 14).
- [24] C. S. Wu et al. 'Experimental Test of Parity Conservation in Beta Decay'. In: *Phys. Rev.* 105 (4 1957), pp. 1413–1415. doi: [10.1103/PhysRev.105.1413](https://doi.org/10.1103/PhysRev.105.1413) (cited on page 14).
- [25] Peter W. Higgs. 'Broken Symmetries and the Masses of Gauge Bosons'. In: *Phys. Rev. Lett.* 13 (16 1964), pp. 508–509. doi: [10.1103/PhysRevLett.13.508](https://doi.org/10.1103/PhysRevLett.13.508) (cited on page 18).
- [26] P.W. Higgs. 'Broken symmetries, massless particles and gauge fields'. In: *Physics Letters* 12.2 (1964), pp. 132–133. doi: [https://doi.org/10.1016/0031-9163\(64\)91136-9](https://doi.org/10.1016/0031-9163(64)91136-9) (cited on page 18).
- [27] F. Englert and R. Brout. 'Broken Symmetry and the Mass of Gauge Vector Mesons'. In: *Phys. Rev. Lett.* 13 (9 1964), pp. 321–323. doi: [10.1103/PhysRevLett.13.321](https://doi.org/10.1103/PhysRevLett.13.321) (cited on page 18).
- [28] Hideki Yukawa. 'On the Interaction of Elementary Particles. I'. In: *Progress of Theoretical Physics Supplement* 1 (Jan. 1955), pp. 1–10. doi: [10.1143/PTPS.1.1](https://doi.org/10.1143/PTPS.1.1) (cited on page 21).
- [29] Nicola Cabibbo. 'Unitary Symmetry and Leptonic Decays'. In: *Phys. Rev. Lett.* 10 (12 1963), pp. 531–533. doi: [10.1103/PhysRevLett.10.531](https://doi.org/10.1103/PhysRevLett.10.531) (cited on page 23).
- [30] Makoto Kobayashi and Toshihide Maskawa. 'CP Violation in the Renormalizable Theory of Weak Interaction'. In: *Prog. Theor. Phys.* 49 (1973), pp. 652–657. doi: [10.1143/PTP.49.652](https://doi.org/10.1143/PTP.49.652) (cited on page 23).
- [31] Ling-Lie Chau and Wai-Yee Keung. 'Comments on the Parametrization of the Kobayashi-Maskawa Matrix'. In: *Phys. Rev. Lett.* 53 (19 1984), pp. 1802–1805. doi: [10.1103/PhysRevLett.53.1802](https://doi.org/10.1103/PhysRevLett.53.1802) (cited on page 23).
- [32] S. L. Glashow, J. Iliopoulos, and L. Maiani. 'Weak Interactions with Lepton-Hadron Symmetry'. In: *Phys. Rev. D* 2 (7 1970), pp. 1285–1292. doi: [10.1103/PhysRevD.2.1285](https://doi.org/10.1103/PhysRevD.2.1285) (cited on page 24).

- [33] *Standard Model Summary Plots June 2021*. Tech. rep. All figures including auxiliary figures are available at <https://atlas.web.cern.ch/Atlas/GROUPS/PHYSICS/PUBNOTES/ATL-PHYS-PUB-2021-032>. Geneva: CERN, 2021 (cited on page 26).
- [34] ATLAS Collaboration. ‘A detailed map of Higgs boson interactions by the ATLAS experiment ten years after the discovery’. In: *Nature* 607.7917 (2022), pp. 52–59. doi: [10.1038/s41586-022-04893-w](https://doi.org/10.1038/s41586-022-04893-w) (cited on page 27).
- [35] *Top working group cross-section summary plots June 2022*. Tech. rep. All figures including auxiliary figures are available at <https://atlas.web.cern.ch/Atlas/GROUPS/PHYSICS/PUBNOTES/ATL-PHYS-PUB-2022-031>. Geneva: CERN, 2022 (cited on page 29).
- [36] K. Abe et al. ‘Atmospheric neutrino oscillation analysis with external constraints in Super-Kamiokande I-IV’. In: *Physical Review D* 97.7 (2018). doi: [10.1103/physrevd.97.072001](https://doi.org/10.1103/physrevd.97.072001) (cited on page 30).